OAK RIDGE NATIONAL LABORATORY
operated by
UNION CARBIDE CORPORATION
for the
U. S. ATOMIC ENERGY COMMISSION

ORNL - TM - 3202

1

THE ANALYSIS OF CREEP DATA IN THE SELECTIONS OF MATERIALS FOR THERMIONIC CAPSULES

R. L. Stephenson

NOTICE This document contains information of a preliminary nature and was prepared primarily for internal use at the Oak Ridge National Laboratory. It is subject to revision or correction and therefore does not represent a final report.

ORNL-TM-3202

Contract No. W-7405-eng-26

METALS AND CERAMICS DIVISION

THE ANALYSIS OF CREEP DATA IN THE SELECTIONS OF MATERIALS FOR THERMIONIC CAPSULES

R. L. Stephenson

Paper presented at the 1969 Conversion Specialist Conference held in Carmel, California, October 21–23, 1969

NOVEMBER 1970

OAK RIDGE NATIONAL LABORATORY
Oak Ridge, Tennessee
operated by
UNION CARBIDE CORPORATION
for the
U.S. ATOMIC ENERGY COMMISSION

CONTENTS

	Page
Abstract	1
Introduction	1
General Considerations	1
Material Properties	5
Conclusions	10
Acknowledgment	10

THE ANALYSIS OF CREEP DATA IN THE SELECTIONS OF MATERIALS FOR THERMIONIC CAPSULES

R. L. Stephenson

ABSTRACT

The creep-rupture properties of arc-melted tungsten, W-5% Re, W-26% Re, W-25% Re-30% Mo, and chemically vapor deposited (CVD) tungsten were studied with a view toward the selection of optimum materials for isotope containment for thermionic capsules. The times to 1, 2, and 5% creep are presented along with the time to rupture as a function of stress. The interaction of various failure criteria is discussed with reference to the selection of allowable stresses.

INTRODUCTION

The concept of enclosing a heat source, either a reactor fuel element or an isotope, in a capsule and producing electricity by thermionic conversion appears attractive for many applications. The integrity of such a device depends on the maintenance of a small space between an emitter and a collector. The attainment of some small strain in the emitter usually limits the design stress. The emitter may constitute the end of a capsule. In other cases the cylindrical sides of a capsule serve as the emitter in which case this is an even more severe limitation. This report discusses the need to consider secondary failure criteria in determining a design stress.

GENERAL CONSIDERATIONS

Let us first consider how creep data are obtained and some of the common ways of displaying creep data. Figure 1 shows schematically several methods of displaying creep data. The classical form of a creep curve is shown in Fig. 1(a). The specimen is held at constant

ORNL-DWG 68-14227

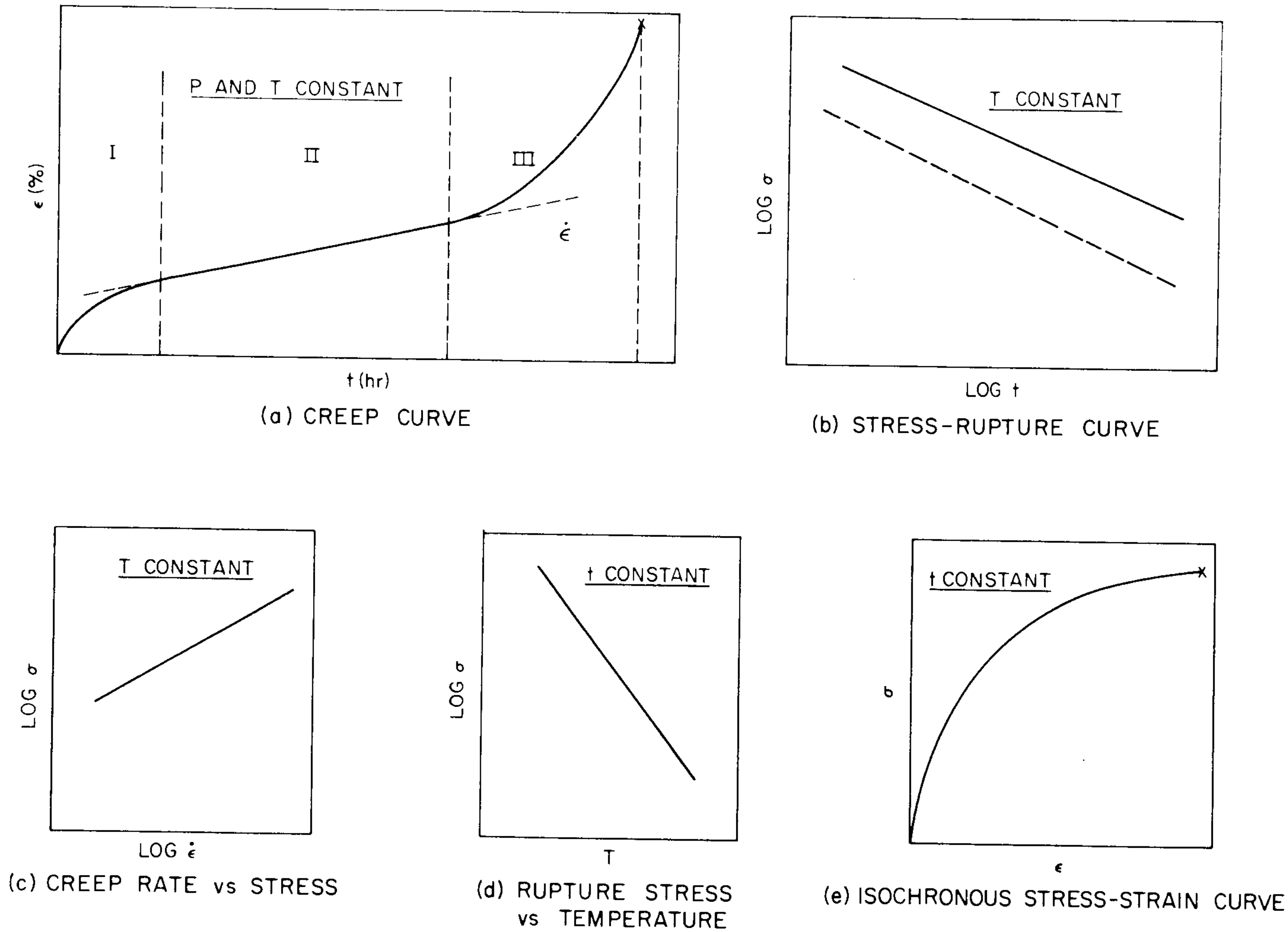

Fig. 1. Schematic Representation of Common Methods for the Display of Creep Data.

temperature (T) and constant load (P) (constant nominal stress), while elongation is recorded as a function of time (t). Although many exceptions are found, a typical creep curve can be divided into three principal regions, primary creep (I), where the curve is concave downward; secondary creep (II), where the curve is roughly linear; and tertiary creep (III), where the curve is concave upward until terminated by fracture. Frequently the logarithms of the rupture times for several creep tests are plotted as a function of the logarithm of the stress (σ) to form a stress-rupture curve as illustrated by the solid line in Fig. 1(b). The times to reach a selected percent strain (ϵ) are sometimes plotted as a function of stress in the same manner as illustrated by the dotted line in Fig. 1(b). One might also plot the secondary creep rate [i.e., the minimum slope ($\dot{\epsilon}$) of the creep curve] as a function of stress on a logarithmic plot. Such a plot is illustrated in Fig. 1(c). It is frequently useful to compare materials by plotting the logarithm of the stress to produce rupture in a specified time (e.g., stress to produce rupture in 1000 hr) versus temperature, as shown in Fig. 1(d). Alternatively one might plot the stress to produce a selected strain in a specified time or the stress to produce a specified secondary creep rate as a function of temperature. Finally, an isochronous stress-strain curve [illustrated in Fig. 1(e)] is useful in establishing design stresses. As the name implies, the stress is plotted as a function of strain at constant time and temperature. For example, the stress to produce 1% creep in 1000 hr, the stress to produce 2% creep in 1000 hr, the stress to produce 3% creep in 1000 hr, etc. (at a given temperature) are plotted with the corresponding stresses. This plot enables one to visualize the effect of changing the design criteria on the design stress.

At this point it should be emphasized that the various parameters taken from the creep curve are only obscurely related. Consider Fig. 2 which shows three schematic creep curves. All three have the same rupture life but the time to a selected strain (ϵ_1) varies widely. Similarly, two curves have the same secondary creep rate while the third had a much smaller creep rate ($\dot{\epsilon}_1 = \dot{\epsilon}_2 \gg \dot{\epsilon}_3$). Such differences and others are experimentally observed.

ORNL-DWG 68-14226R

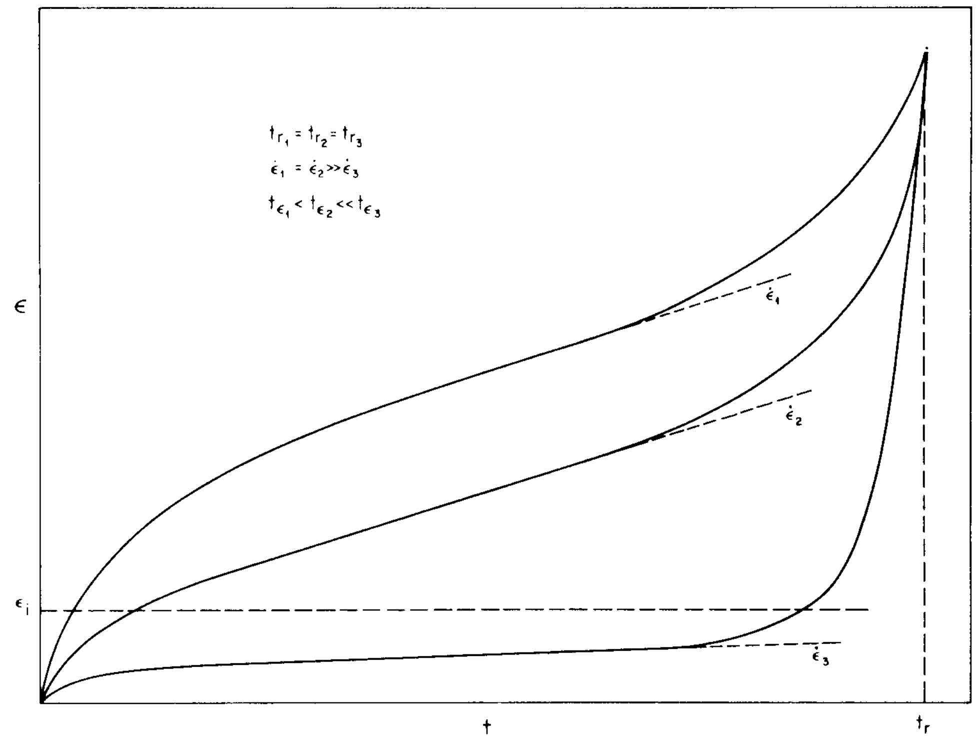

Fig. 2. Schematic Creep Curves with Identical Rupture Times.

Design stresses are usually chosen on the basis of some primary design criterion. In the case of a thermionic capsule, the stress to produce some specified strain in the design life might well serve as such a criterion. A design stress usually reflects the consideration of one or more secondary design criteria. For example, one may decide that the design stress must not exceed some fraction of the rupture stress. These criteria interact to such an extent that a design stress cannot be selected on the basis of one without recourse to the others. This point can be illustrated with the experimental data to follow.

MATERIAL PROPERTIES

In Fig. 3 the times to selected percent strain and to rupture are plotted as a function of stress at 1650°C for unalloyed, arc-melted tungsten. Similar data are shown for arc-melted W–5% Re, W–26% Re, W–25% Re–30% Mo, and for CVD tungsten in Figs. 4 through 7, respectively.

The arc-melted materials were received in the form of wrought rods. The CVD tungsten was recently produced, low fluorine material (5 to 10 ppm F) deposited in the form of large sheets. All specimens were held 1 hr at temperature prior to loading and tested at pressures $\leq 4 \times 10^{-7}$ torr.

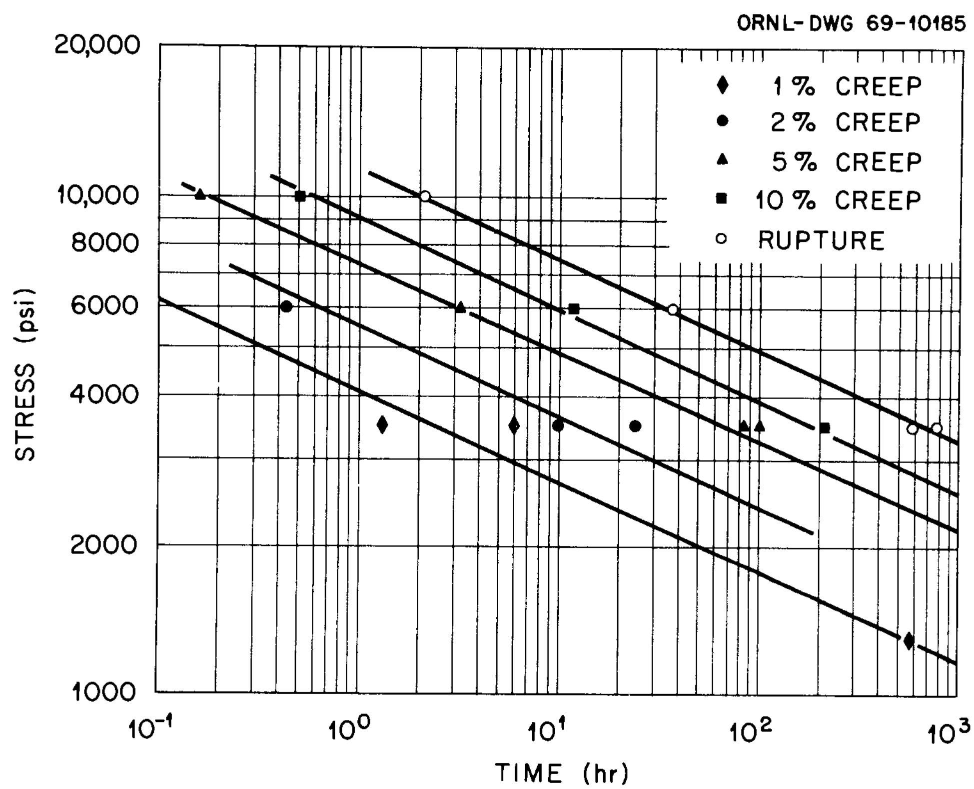

Fig. 3. Creep-Rupture Properties of Unalloyed, Arc-Melted Tungsten at 1650°C.

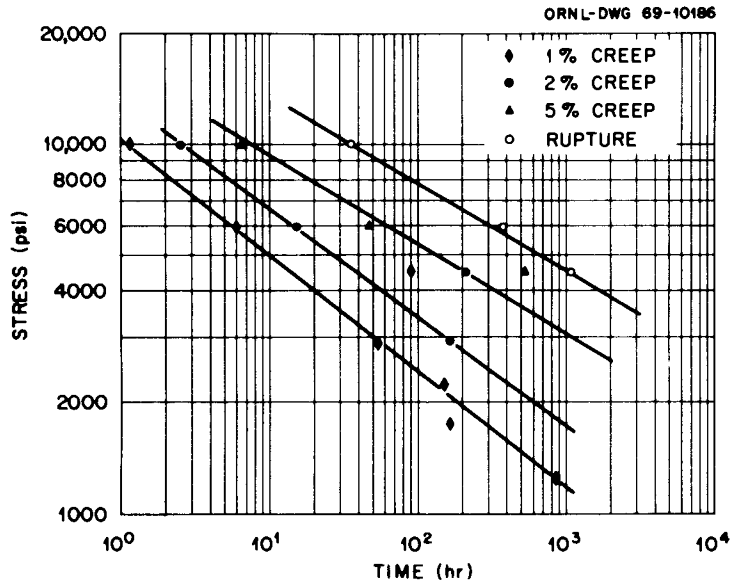

Fig. 4. Creep-Rupture Properties of W–5% Re at 1650°C.

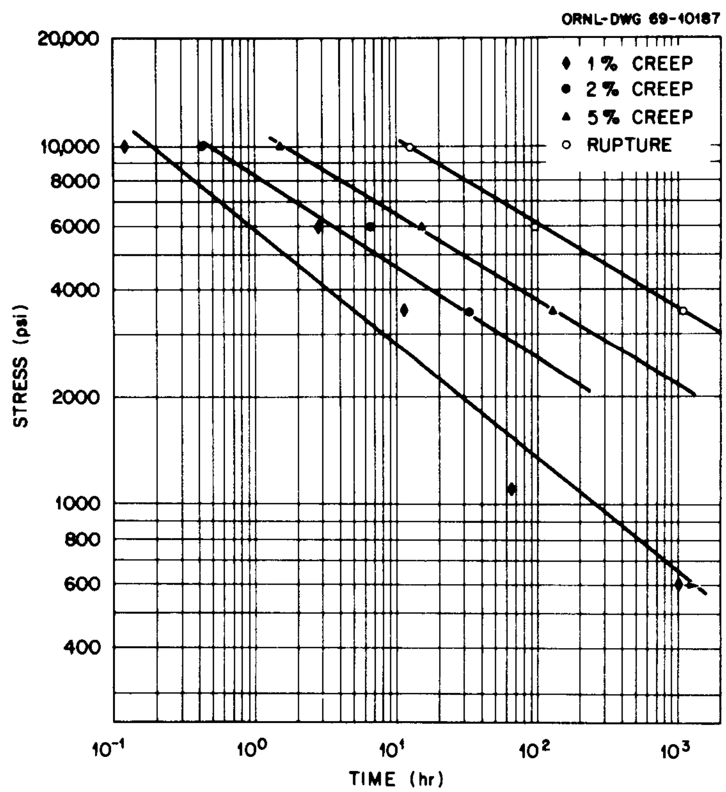

Fig. 5. Creep-Rupture Properties of W–26% Re at 1650°C.

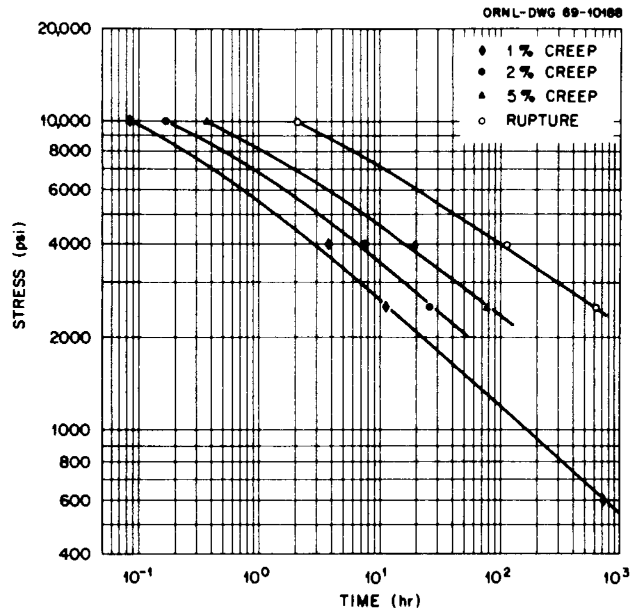

Fig. 6. Creep-Rupture Properties of W–25% Re–30% Mo at 1650°C.

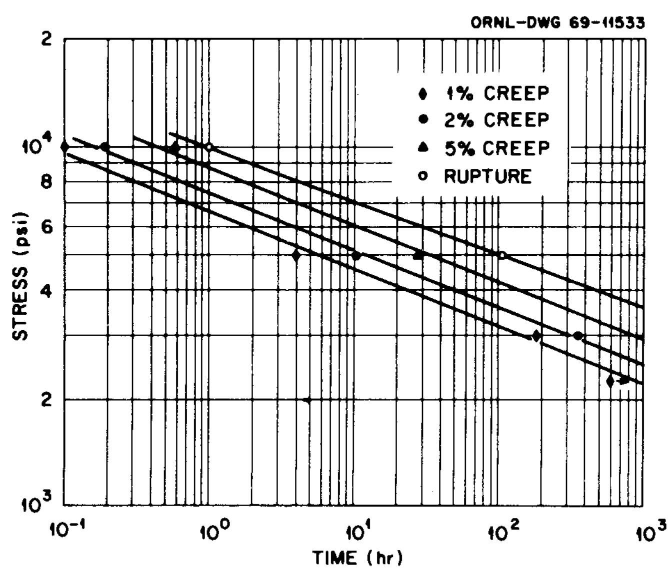

Fig. 7. Creep-Rupture Properties of Chemically Vapor Deposited Tungsten at 1650°C.

Let us assume that the primary failure criterion for a thermionic capsule is the attainment of 1% creep. Since we must avoid the release of radioactive material, let us establish the additional condition that the design stress must not exceed 50% of the stress to produce rupture in the design life.

Figure 8 compares the stress to produce 1% creep in 1000 hr for each of the aforementioned materials. On this basis CVD tungsten seems superior, followed by W–5% Re, then unalloyed tungsten. One is able to visualize the interaction of failure criteria much better, however, when the materials are compared using isochronous stress-strain curves as in Fig. 9. It is apparent that the stress to produce 1% creep in CVD tungsten exceeds 50% of the rupture stress. This stress is still above the stress to produce 1% creep in W–5% Re but the margin is reduced. If we decide that we can tolerate 2 or 3% strain, the allowable stress for CVD tungsten does not increase since it is already limited by 50% of the rupture stress. The allowable stress for W–5% Re can be increased, however, making it the most attractive alloy under these conditions. On the other hand, if we decide that 50% of the rupture stress is too conservative and that 80% is more reasonable, the CVD tungsten becomes most attractive again.

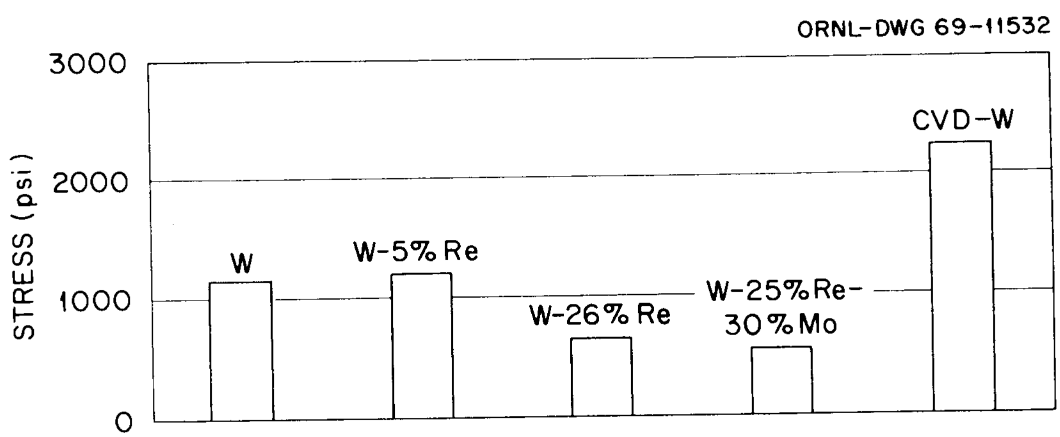

Fig. 8. Stress to Produce 1% Creep in 1000 hr for Selected Tungsten-Base Materials at 1650°C.

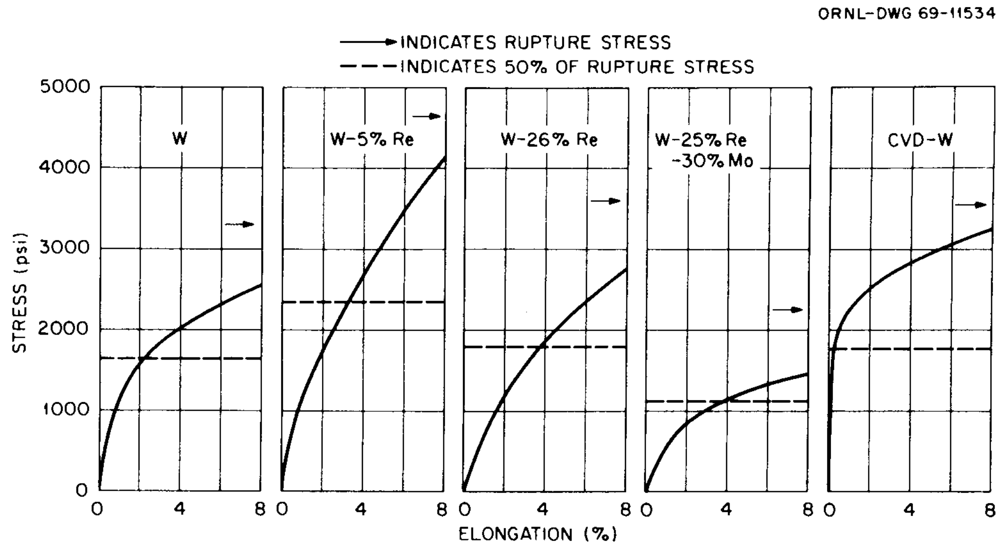

Fig. 9. Isochronous Stress-Strain Curves Comparing Stress to Produce 1% Creep in 1000 hr for Selected Tungsten-Base Materials at 1650°C.

Similarly, the effect of thermomechanical history cannot be treated in isolation. Figure 10 shows 50-hr isochronous stress-strain curves for powder-metallurgy W–25% Re in two conditions. The stresses to produce low strains have been roughly doubled by annealing at 2200°C, but the rupture stress was not changed. Hence, it is unlikely that one can take full advantage of this increase.

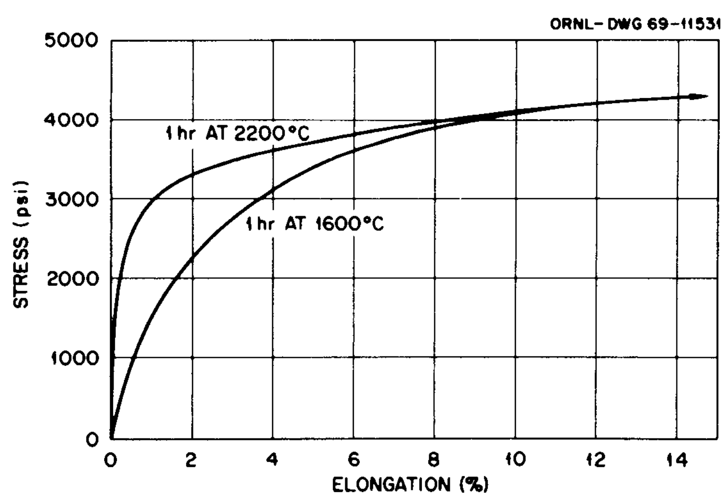

Fig. 10. Isochronous Stress-Strain Curves Comparing Stress to Produce 1% Creep in 50 hr in Powder-Metallurgy W–25% Re at 1650°C.

CONCLUSIONS

In conclusion, several points should be emphasized. Attention must not be focused on one aspect of material behavior to the exclusion of others. A complete understanding of a particular material's behavior at various stresses and temperatures is necessary before safe design is possible. This is particularly important in isotopic capsules since they will see changing temperatures and stresses. Finally, the data presented here do not constitute design data. Material properties must be expected to vary from heat to heat. The properties of several heats must be characterized for sufficient time to permit the construction of isochronous stress-strain curves for the design life without unreasonable extrapolation.

ACKNOWLEDGMENT

The author wishes to acknowledge the contributions made to this work by others. Those who merit specific mention are J. I. Federer for production of the CVD tungsten, R. E. McDonald for procurement and fabrication of the arc-melted materials, E. B. Patton for performance of the experimental details, R. W. Swindeman and A. C. Schaffhauser for review of the manuscript, H. E. McCoy and J. R. Weir for valuable suggestions and guidance during the course of the work, and the Metals and Ceramics Division Reports Office for the preparation of the manuscript.

INTERNAL DISTRIBUTION

1–3. Central Research Library
4. ORNL – Y-12 Technical Library Document Reference Section
5–14. Laboratory Records Department
15. Laboratory Records, ORNL RC
16. ORNL Patent Office
17. G. M. Adamson, Jr.
18. D. T. Bourgette
19. D. A. Canonico
20. K. V. Cook
21. F. L. Culler
22. J. E. Cunningham
23. J. H. DeVan
24. J. R. DiStefano
25. R. G. Donnelly
26. J. I. Federer
27. J. H Frye, Jr.
28. J. L. Gregg
29. W. O. Harms
30–32. M. R. Hill
33. H. Inouye
34. D. H. Jansen
35. J. W. Koger
36. R. W. McClung
37. H. E. McCoy, Jr.
38. R. E. McDonald
39. D. L. McElroy
40. P. Patriarca
41. G. A. Reimann
42. J. L. Scott
43. A. C. Schaffhauser
44. C. E. Sessions
45. G. M. Slaughter
46–60. R. L. Stephenson
61. D. A. Sundberg
62. R. W. Swindeman
63. D. B. Trauger
64. S. C. Weaver
65. J. R. Weir, Jr.

EXTERNAL DISTRIBUTION

66. D. F. Cope, RDT, SSR, AEC, Oak Ridge National Laboratory
67. G. K. Dicker, AEC, Washington
68. R. Hall, NASA, Lewis Research Center
69. H. Kato, U.S. Department of the Interior, Bureau of Mines Albany, Oregon
70. T. A. Moss, NASA, Lewis Research Center
71. N. D. Sanders, NASA, Lewis Research Center
72. H. Schwartz, NASA, Lewis Research Center
73. F. C. Schwenk, AEC, Washington
74. J. M. Simmons, Division of Reactor Development and Technology, AEC, Washington
75. A. Van Echo, AEC, Washington
76. G. W. Wensch, AEC, Washington
77. Laboratory and University Division, AEC, Oak Ridge Operations
78–92. Division of Technical Information Extension